

Solutions For Homework #8

Problem 1:[10 pts]

- (a) In this problem, the circular aperture functions representing Polyphemus' and Odysseus' eyes are expressed as functions of the unitless independent variable $r_\lambda = \frac{r}{\lambda}$, where λ is the wavelength of $0.5 \mu\text{m}$. Polyphemus' eye can be modeled as a uniformly-illuminated circular aperture, of diameter $\frac{10 \text{ cm}}{\lambda} = 200,000$ wavelengths.

$$f_{Polyphemus}(r_\lambda) = \text{rect}\left(\frac{r_\lambda}{200000}\right) \quad (1)$$

Odysseus' eyes can each be modeled as a uniformly-illuminated round aperture of diameter $\frac{1 \text{ cm}}{\lambda} = 20,000$ wavelengths,

$$f_{Odysseus}(r_\lambda) = \text{rect}\left(\frac{r_\lambda}{20000}\right) \quad (2)$$

The impulse responses are the far-field power patterns of the individual apertures, which in turn are proportional to the squared-magnitude of the Fourier Transform of the individual aperture illumination functions

$$\begin{aligned} P_{Polyphemus} &= \left| \int_0^\infty f_{Polyphemus}(r_\lambda) J_0\left(2\pi\frac{\theta}{\lambda}r\right) r dr \right|^2 \\ &= 20000^4 \text{jinc}^2(200000 \theta) \end{aligned}$$

where, in the above, we make a change of variables $r_\lambda = \frac{r}{\lambda}$. Similarly,

$$P_{Odysseus} = 20000^4 \text{jinc}^2(20000 \theta) \quad (3)$$

Figure 1 illustrates the definition of the angle θ . Under the small-angle approximation, we assume that θ in Figure 1 can be related to the angles ϕ and γ as follows

$$\theta^2 \approx \phi^2 + \gamma^2 \quad (4)$$

The angles ϕ and γ can be interpreted as azimuth and elevation (in spherical coordinate terminology) or longitude and latitude respectively. Due to

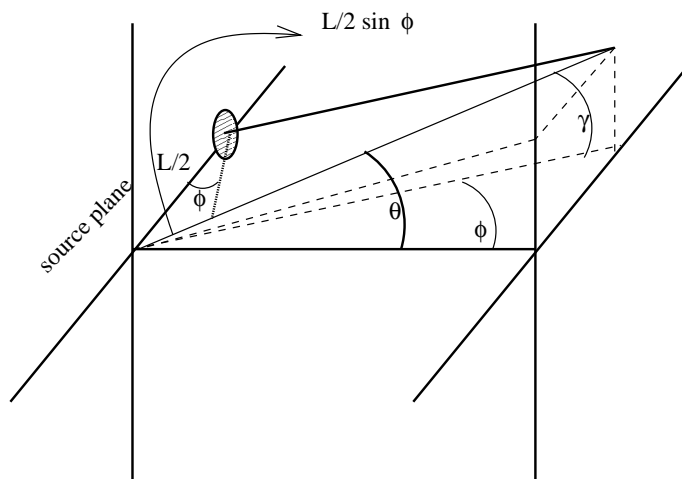


Figure 1:

the circular symmetry of the aperture illumination function, the impulse response is also rotationally-symmetric with its argument, θ being defined as shown in the figure. Figure 2 plots the impulse responses of Polyphemus' and each of Odysseus' eyes. As Odysseus' eye is 10 times smaller than Polyphemus', its impulse response is 10 times broader, as is shown in Figure 2. We would expect Polyphemus' eye to have a width of 0.0007 degrees by recalling that the width of the mainlobe of the jinc-function response is equal to $2 \times 1.22 \frac{1}{200000} \times 180/\pi = 0.000699$ degrees.

- (b) The transfer function for each eye is the autocorrelation of the eye's aperture illumination function. Put another way, the transfer function is the Fourier Transform of the aperture (power) impulse responses. As the transfer function and impulse response form a Fourier Transform pair, their arguments must have reciprocal units. We know that the far-field power patterns (i.e. the impulse responses) of the apertures are a function of θ with units of radians. Therefore, the units of the argument of the transfer function should be reciprocal, i.e. cycles per radians. Furthermore, we expect the transfer function to be circularly symmetric since the impulse response possesses rotational symmetry. Consequently,

$$p_{Polyphemus} = 200000^2 \text{ chat} \left(\frac{q}{200000} \right)$$

$$p_{Odysseus} = 20000^2 \text{ chat} \left(\frac{q}{20000} \right)$$

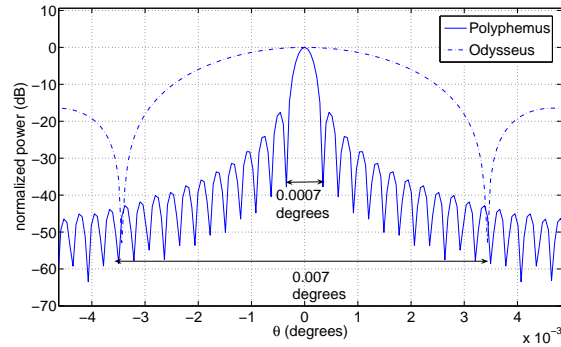


Figure 2:

where $q = \sqrt{u^2 + v^2}$ has units of cycles/radians. The function *chat* is the Chinese Hat function, defined as

$$\text{chat}(q) = \frac{1}{2}(\cos^{-1} |q| - |q|\sqrt{1 - q^2})\text{rect}(0.5q) \quad (5)$$

The transfer functions for each of Odysseus' eyes and Polyphemus' eye is shown in Figure 3.

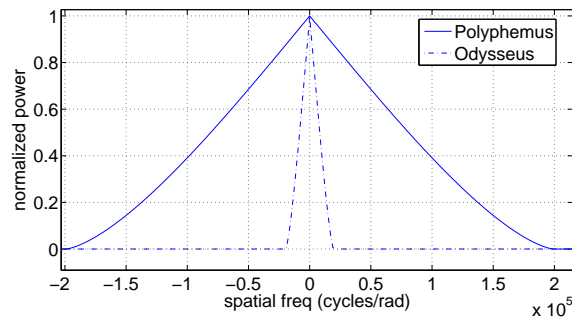


Figure 3:

- (c) Let $F_0(\theta)$ be the far-field amplitude pattern (as opposed to power-pattern) of an aperture. We know that $F_0(\theta)$ and the aperture illumination function form a Fourier Transform pair. This function describes the amplitude and

phase of the (say, electric) field in the far-field. By the reciprocity theorem of antennas, this amplitude pattern also describes the weighting - as a function of angle - applied to waves incident on the aperture.

Each of Odysseus' eyes has an *element pattern* given by

$$F_0\left(\frac{\theta}{\lambda}\right) = 20000^2 \text{jinc}(20000\theta) \quad (6)$$

The eyes are separated by 20000 wavelengths. An interferometric combination of signals (waves) received at both eyes would yield a total signal

$$\begin{aligned} F(\theta) &= F_0(\theta) \left(e^{j\frac{2\pi}{\lambda} \frac{L}{2} \sin\phi} + e^{-j\frac{2\pi}{\lambda} \frac{L}{2} \sin\phi} \right) \\ &= 2F_0(\theta) \cos(\pi L_\lambda \sin\phi) \\ &\approx 2F_0(\theta) \cos(\pi L_\lambda \phi) \end{aligned}$$

where $L_\lambda = \frac{L}{\lambda}$, the separation of Odysseus' eyes in terms of number of wavelengths. In the above, $F(\theta)$ gives the amplitude response to a point source at angle θ . Further, we note that additional phase delays associated with signals incident on each of Odysseus' eyes depend on ϕ . This is because, with reference to Figure 1, Odysseus' eyes are displaced horizontally causing the extra phase delays of waves to depend on the azimuth angle ϕ only, as shown in Figure 1. Of course, the far-field power pattern resulting from interferometrically combining the signals at the two eyes is simply the squared-magnitude of this effective amplitude pattern,

$$\begin{aligned} P_{Odysseus,int} &= 4 \times 20000^4 \text{jinc}^2(20000\theta) \cos^2(\pi L_\lambda \phi) \\ &= 2 \times 20000^4 \text{jinc}^2(20000\theta) [1 + \cos(2\pi L_\lambda \phi)] \end{aligned}$$

The new transfer function is the Fourier Transform of the far-field power pattern $P_{Odysseus,int}$ above,

$$p_{Odysseus,int} = 2 \times 20000^2 \text{chat}\left(\frac{q}{20000}\right) ** [\delta(u, v) + \delta(u - L_\lambda, v) + \delta(u + L_\lambda, v)] \quad (7)$$

The transfer function of the pair of Odysseus' eyes is shown in Figure 4 along with the transfer function of Polyphemus' eye. As can be seen from Figure 4, the interferometric combination of signals received at both of Odysseus' eyes allows him to have additional sensitivity to high spatial frequency energy. However, due to the fact that Odysseus' eyes are 10 times smaller than Polyphemus', the transfer function widths are correspondingly small.

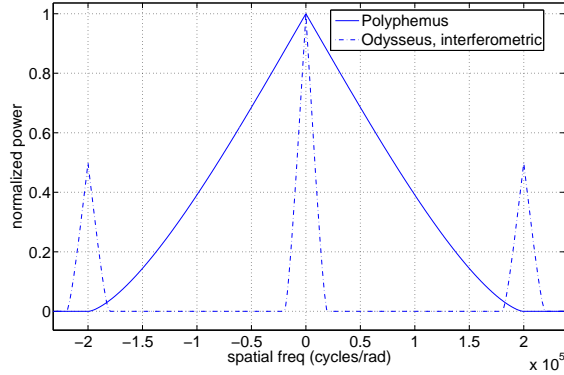


Figure 4:

(d) Odysseus could rotate his head to obtain more spectral coverage.

Problem 2:[10 pts]

This is a Fourier synthesis problem. To recover the intensity distribution of the object, we need to form a weighted sum of complex exponentials. The weights in the sum are the complex Fourier amplitudes from the data file *hw8prob2data*, while the frequencies of the complex exponentials in the sum are derivable from the interferometer baseline spacings in the same data file.

Why is this the case? Recall from Handout #34 that the **complex visibility** of a 2-element correlating interferometer, illuminating the sky in some direction θ_0 is related to Fourier decomposition of the target's brightness distribution:

$$V(v_0) = \int b(x + \theta_0) e^{-j2\pi v_0 x} dx \quad (8)$$

where $v_0 = \frac{L}{\lambda} \cos(\theta)$ and L is the interferometer baseline spacing. The integral above describes a Fourier decomposition of the brightness distribution $b(x)$ of the target into a weighted sum of complex exponentials. The left-hand side in the above describes the weighting applied to the complex exponential $e^{-j2\pi v_0 x}$ in that sum, and that weight is exactly the complex visibility. Thus, if we knew the "spectrum" of the target's brightness distribution - i.e. its complex visibilities for all v_0 - we could, in principle, recover the object's brightness distribution $b(x)$

exactly by the following integral:

$$b(x) = \int V(v_0) e^{j2\pi v_0 x} dv_0 \quad (9)$$

which is, essentially, a sum of complex exponentials weighted by complex visibility values.

Let us assume that the interferometer is pointed vertically, so that $\theta_0 = 0$. Then, the transform variable $v_i = \frac{L_i}{\lambda}$ varies according to baseline spacing L_i . We are told that the given values of interferometer baseline is unitless, as we would expect the transform variable v_i to be. Thus, we take the unitless values contained in the first column in data file *hw8prob2data* to represent different values of v_i , the transform variable. We synthesize the brightness distribution of the target as follows

$$b(x) = \sum_i V_i e^{-j2\pi \frac{v_i x}{N}} \quad (10)$$

In the above, x denotes the spatial axis of the brightness function $b(x)$; it is an array of length $N = 256$. The sum runs over the number of different interferometer baseline spacings in the data file *hw8prob2data*. Figure 5 shows the result.

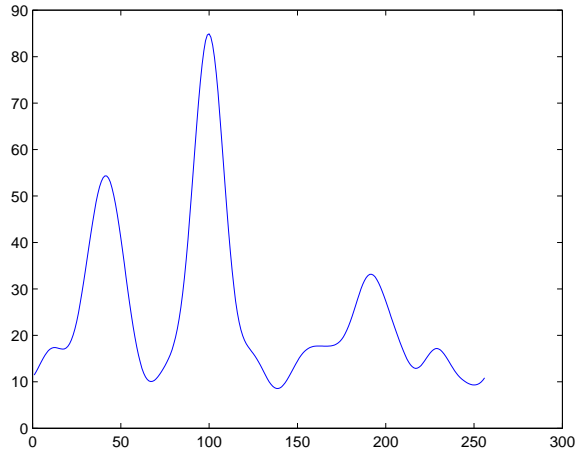


Figure 5:

Problem 3:[10 pts]

- (a) The geometry of this problem is similar to that in Problem 1, except that the elevation angle γ is used here instead of azimuth ϕ . To see this, refer to Figure 6 which shows a mirror image of the antenna located a distance $2H$ below the aperture seated on the edge of the cliff. The path length difference Δx between the direct ray and reflected ray, from geometry, is

$$\Delta x = \frac{H}{\sin \gamma} - \left(\frac{H}{\sin \gamma} - 2H \sin \gamma \right) = 2H \sin \gamma \quad (11)$$

This difference in path length is exactly equal to the path difference of

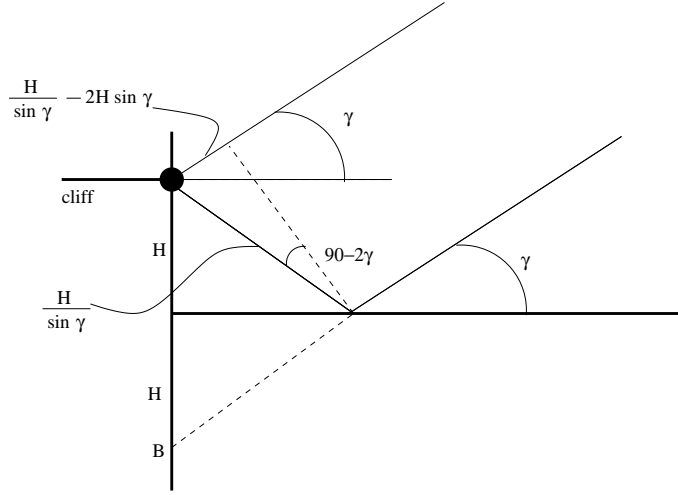


Figure 6:

two rays, one incident at the antenna on the cliff and the other at a mirror image point B as shown in Figure 1. Combining the direct and reflected signal would thus be equivalent to interferometrically combining signals at the two apertures vertically spaced by $2H$. Following Problem 1, we would expect a far-field amplitude pattern resulting from the total signal as follows

$$\begin{aligned} F(\theta) &= F_0(\theta) \left(e^{j\frac{2\pi}{\lambda} \frac{2H}{2} \sin \gamma} + e^{-j\frac{2\pi}{\lambda} \frac{2H}{2} \sin \gamma} \right) \\ &= 2F_0(\theta) \cos \left(2\pi H \frac{\sin \gamma}{\lambda} \right) \\ &\approx 2F_0(\theta) \cos(2\pi H_\lambda \gamma) \end{aligned}$$

where $F_0\left(\frac{\theta}{\lambda}\right)$ is the far-field element pattern arising of the circular aperture of diameter $\frac{8\text{m}}{\lambda} = 4$ wavelengths and, as before, $H_\lambda = \frac{H}{\lambda}$. That is,

$$F_0(\theta) = 4^2 \text{jinc}(4\theta) \quad (12)$$

Consequently, the far-field power pattern of this early interferometer is given by

$$P(\phi, \gamma) = 4 \times 4^4 \text{jinc}^2(4\theta) \cos^2(2\pi H_\lambda \gamma) \quad (13)$$

where, as before, the small angle approximation gives $\theta^2 \approx \phi^2 + \gamma^2$. We see that the elevation-dependent component of the total power pattern destroys the circular symmetry due to the round aperture. Now, the transfer function of this early interferometer is given by the Fourier Transform of the far-field power pattern. Thus,

$$p(u, v) = 2 \times 4^2 \text{rect}\left(\frac{q}{4}\right) ** [\delta(u, v) + \delta(u, v - 2H_\lambda) + \delta(u, v + 2H_\lambda)] \quad (14)$$

where $q = \sqrt{u^2 + v^2}$. Figure 7 shows a comparison of the transfer function of the original circular aperture with that of the interferometer. As we can see, the interferometer has a nonzero response in *vertical* spatial frequencies around 0 meters and ± 400 cycles/rad. This additional spectral response in the vertical v direction is due to the elevation-dependent interferometric combination of the direct and reflected signals. In contrast to the response of the circular aperture, which is centered at the origin and has a width of about 8 cycles/rad.

- (b) We observe from Figure 7 that the transfer function of the interferometer is zero for spatial frequencies in the range from 10 cycles/rad to about 390 cycles/rad. This implies that sinusoidal components of the form $e^{-j2\pi L_\lambda \gamma}$ for $10 < L < 390$ cycles/rad in the target's brightness distribution would be effectively invisible to the interferometer. Similarly, sinusoidal components with spatial frequencies in the azimuth direction greater than about 10 meters would also appear invisible to the interferometer.
- (c) Parts (a) and (b) assume that the sea is a flat, mirror-like surface that reflects incoming radiation at an angle equal to the incident angle. Random waves on the ocean surface will effectively tilt the surface at an angle from the horizontal dependent on the rms roughness of the sea. In the presence of a rough sea, the response of the interferometer will be

$$P(\phi, \gamma) = [2 \times 4^2 \text{jinc}(4\theta) \cos(2\pi H_{\lambda}(\gamma - \alpha))]^2 \quad (15)$$

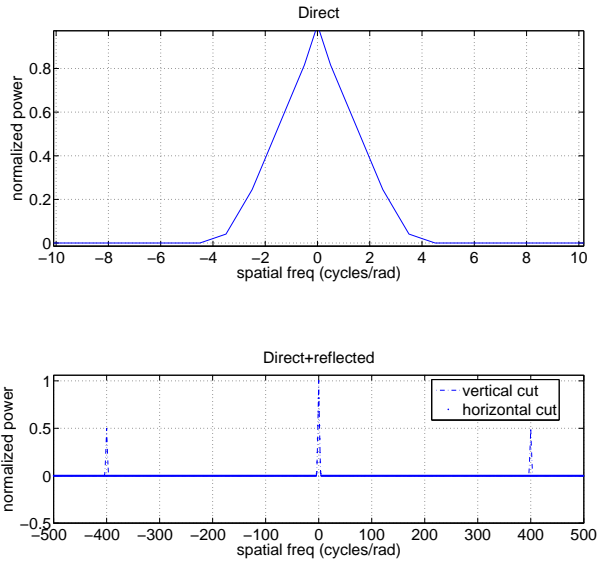


Figure 7:

where α is the tilt angle caused by waves at the reflection point and $\theta^2 \approx \gamma^2 + \phi^2$, as before. Knowing the elevation of the incoming radiation, γ , we would measure the above intensity response and deduce the local angle α . Of course, this measurement would have to be performed repeatedly over time, and an average value of rms sea surface roughness could be deduced.

Problem 4:[10 pts]

The spectral coverage of the aperture array is determined by its 2D autocorrelation function. The autocorrelation function is also the 2D transfer function whose support determines the spatial frequency passband of the system. We compute the autocorrelation of the aperture array numerically. Figure 8 shows the aperture array, where we assume uniform illumination on each of the rectangular apertures. We are not given a coordinate system, and so we take the top left hand corner to be the origin.

Figure 9 shows a contour map of the 2D autocorrelation of the aperture array. The horizontal and vertical axis are spatial frequency. The individual rectangular-like segments are, in fact, lazy pyramid functions, as shown in Figure 10. This

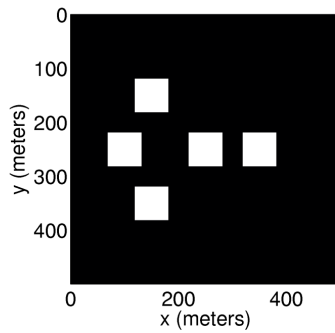


Figure 8:

function is the result of correlating a 2D rect function with itself. Figure 9 shows

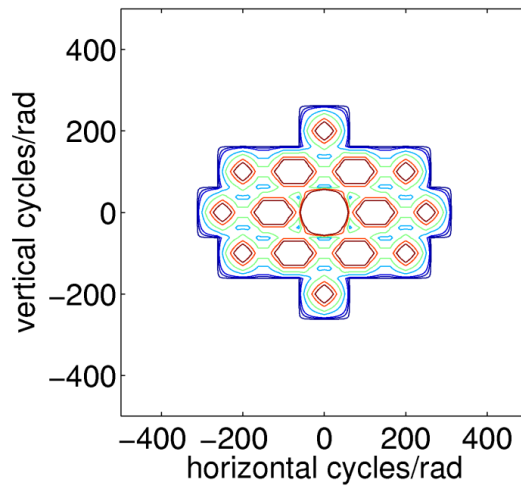


Figure 9:

the extent of the $u - v$ plane covered by the transfer function of the aperture array. The MATLAB code for this problem is given at the back.

Problem 5:[10 pts]

(a) This problem involves convolving the brightness distribution given in the

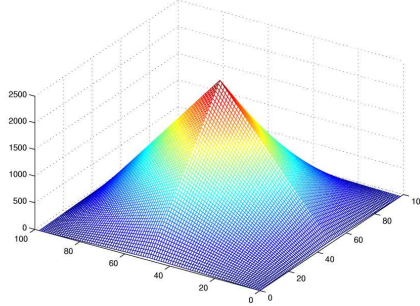


Figure 10:

data file *hw8prob5data* with impulse responses derived from a circular aperture as well as from the antenna array shown in Problem 4.

We first note that we are told that the angular spacing of the discrete-spaced brightness distribution of the target, here termed $\Delta\phi = \Delta\gamma = 71.5$ millidegrees. Here, ϕ and γ refer to azimuth and elevation angles for locating objects in the sky. Knowing the angular spacing allows us to derive the spacing $\Delta x, \Delta y$ between grid points in the spatial domain, thereby allowing us to define the aperture functions on a grid. This is done as follows (for the x case; the y case follows similarly):

$$\Delta x_\lambda = \frac{1}{N\Delta\phi} \quad (16)$$

The spacing between grid points in the x spatial dimension, Δx_λ above, is expressed in terms of wavelengths. That is,

$$\Delta x_\lambda = \frac{\Delta x}{\lambda} \quad (17)$$

We could make use of grid spacing in meters following the formula above. However, for this problem, the circular aperture and antenna array are expressed as functions of independent variables $x_\lambda = \frac{x}{\lambda}$ and $y_\lambda = \frac{y}{\lambda}$. The circular aperture is defined as follows

$$f_\circ(r_\lambda) = \text{rect}\left(\frac{r_\lambda}{312.5}\right) \quad (18)$$

where $r_\lambda = \sqrt{x_\lambda^2 + y_\lambda^2}$ and, when the wavelength of radiation is 80 cm, the circular aperture has a diameter of $\frac{250 \text{ m}}{\lambda} = 312.5$ wavelengths. The impulse

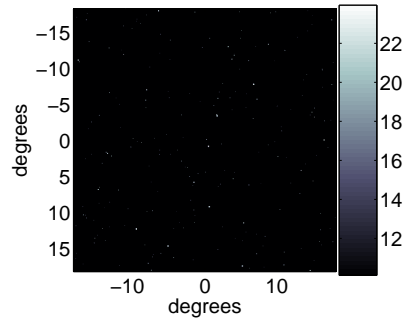


Figure 11:

response of the circular aperture is the squared-magnitude of its element pattern. The element pattern is given by the Fraunhofer integral (a Fourier Transform) of the circular aperture illumination function:

$$\begin{aligned}
 F_{circ}(\theta) &\approx \int_0^\infty f_{circ}(r_\lambda) J_0(2\pi\theta r_\lambda) r_\lambda dr_\lambda \\
 &= 312.5^2 \text{jinc}(312.5 \theta) \\
 \Rightarrow P_{circ}(\theta) &= 312.5^4 \text{jinc}^2(312.5 \theta)
 \end{aligned}$$

where $P_{circ}(\theta)$ denotes the impulse response of the circular aperture. This impulse response is convolved with the brightness distribution obtained from the data file *hw8prob5data* and shown in Figure 11 to obtain an image shown in Figure 12. The circular aperture has a diameter of 250 meters. The

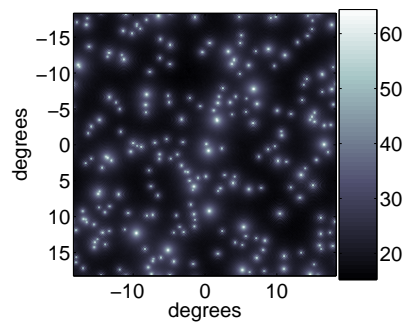


Figure 12:

area in square meters of this aperture is thus $\pi \times \left(\frac{250}{2}\right)^2 = 49,087 \text{ meters}^2$.

- (b) The aperture array shown in Problem 4 and shown in Figure 8 is Fourier-Transformed to give the element pattern (according to the Fraunhofer relationship). Squaring the element pattern's magnitude gives the impulse response, which is convolved with the brightness distribution in Figure 11 to produce an image shown in Figure 13. Each rectangular aperture in the

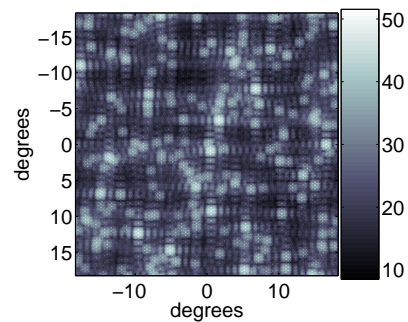


Figure 13:

array has an area of $50 \times 50 = 2500$ meters². Five rectangular apertures comprise the whole array, giving a total area of $5 \times 2500 = 12,500$ meters².

Figures 14 and 15 show the transfer function footprints in the $u - v$ plane of the circular aperture and antenna array respectively. The area in white denotes regions in the $u - v$ plane where the individual antennas produce a non-zero spatial frequency response. By inspection, we can see that the

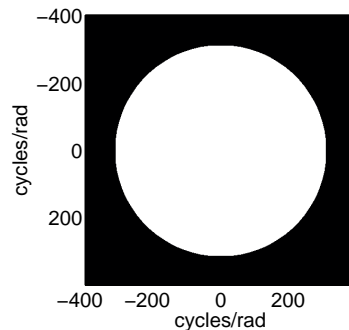


Figure 14:

transfer functions corresponding to both apertures cover the $u - v$ plane

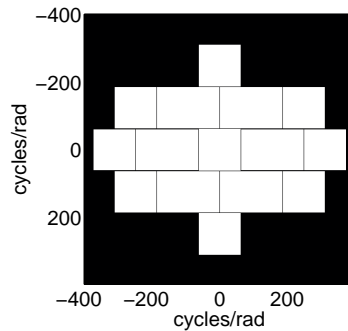


Figure 15:

roughly equally.

MATLAB code for Problem 1

parameters - Note: all distances in units of wavelengths

```

lambda = 0.5e-6;
D_poly = 0.1/lambda;
D_ody = 0.01/lambda;
L = 0.1/lambda;
Delta = 1000;
N = 1000;

% create aperture illumination functions
horiz = [-N/2:N/2-1]*Delta; vert = [-N/2:N/2-1]*Delta;
[x,y] = meshgrid(horiz, vert);
r = sqrt(x.^2 + y.^2);

f_poly = zeros(size(r)); f_poly(find(r<=D_poly/2)) = 1;
f_ody = zeros(size(r)); f_ody(find(r<=D_ody/2)) = 1;

% Part (a)

% Take FFT and find far-field power pattern

```

```

P_poly = fftshift( abs( fft2( fftshift(f_poly) ) ).^2 );
P_ody = fftshift( abs( fft2( fftshift(f_ody) ) ).^2 );

% create azimuth and elevation angles, phi and gamma
horiz_trans_freq = 2*pi*[-N/2:N/2-1]*(1/N)*(1/Delta);
vert_trans_freq = 2*pi*[-N/2:N/2-1]*(1/N)*(1/Delta);

phi = horiz_trans_freq*180/pi/2/pi;
gamma = vert_trans_freq*180/pi/2/pi;

% extract cut horizontally through both power patterns

Pcut_poly = P_poly(N/2+1,:); Pcut_ody = P_ody(N/2+1,:);
% Plot cuts, normalized in amplitude, on dB scale
figure(1);
plot(phi,10*log10(Pcut_poly./max(Pcut_poly)));
hold on;
plot(phi,10*log10(Pcut_ody./max(Pcut_ody)),'-.');
h = gca;set(h,'FontSize',20); xlabel('\theta (degrees)');
ylabel('normalized power (dB)'); grid on;
legend('Polyphemus', 'Odysseus',0);

% Part (b)

% transfer function is Fourier Transform of far-field
% power pattern. Take cuts

Delta_phi = pi/180*(phi(2)-phi(1));
Delta_gamma = pi/180*(gamma(2)-gamma(1));

p_poly = real( fftshift( ifft2( fftshift(P_poly) ) ) );
p_ody = real( fftshift( ifft2( fftshift(P_ody) ) ) );

% create spatial frequency arrays (in cycles/rad) from
% angular arrays Phi and Gamma
u = [-N/2:N/2-1]*(1/N)*(1/Delta_phi);
v = [-N/2:N/2-1]*(1/N)*(1/Delta_gamma);

```

```

pcut_poly = p_poly(N/2+1,:); pcut_ody = p_ody(N/2+1,:);

% Plot cuts, normalized in amplitude,
figure(2);
plot(u,pcut_poly./max(pcut_poly));
hold on;
plot(u,pcut_ody./max(pcut_ody),'-.');
h = gca;set(h,'FontSize',20); xlabel('spatial freq (cycles/rad)');
ylabel('normalized power'); grid on;
legend('Polyphemus', 'Odysseus',0);

% Part (c)

% Multiply Odysseus' element power pattern with cosine-squared
% factor due to the interferometer
P_int_ody =4*P_ody.*...
    cos((L/2).*repmat( horiz_trans_freq,[size(P_ody,1) 1]) ).^2;

p_int_ody = real( fftshift( fft2( fftshift( P_int_ody ) ) ) );
pcut_int_ody = p_int_ody(N/2+1,:);

figure(3);
plot(u,pcut_poly./max(pcut_poly));
hold on;
plot(u,pcut_int_ody./max(pcut_int_ody),'-.');
h = gca;set(h,'FontSize',20); xlabel('spatial freq (cycles/rad)');
ylabel('normalized power'); grid on;
legend('Polyphemus', 'Odysseus, interferometric',0);

```

MATLAB code for Problem 2

```

% load in data file
q = load('hw8prob2data');

% form complex Fourier coefficients (visibilities)
data = q(:,2) + sqrt(-1)*q(:,3);

```

```

% form array of spatial frequencies (interferometer
% baseline spacings)
v = q(:,1);

% create spatial axis of 256 points
x = [0:256-1];

% perform Fourier synthesis of brightness distribution
% recall that brightness is a real quantity
s = 0;
for k = 1:length(v)
    t = data(k)*exp(sqrt(-1)*2*pi*v(k)*x/length(x));
    tconj = data(k)*exp(sqrt(-1)*2*pi*v(k)*(length(x)-x)/length(x));

    s = s + t + tconj;
end

% plot out results - there's a little bit of imaginary part
% left in the sum.
plot(x, real(s));

```

MATLAB code for Problem 5

```

% parameters
lambda = 0.8;
N = 512;
Delta_phi = 71.5e-3*pi/180;
Delta_gamma = Delta_phi;
D = 250/lambda;
w = 50/lambda;

% create angular grid
Phi = [-N/2:N/2-1]*Delta_phi; Gamma = [-N/2:N/2-1]*Delta_gamma;
[phi,gamma] = meshgrid(Phi,Gamma);

% Note: if angular spacing is Delta (in radians)

```

```

% then  $1/N/\Delta_x = \Delta \Rightarrow \Delta_x = 1/N/\Delta$  in units of
% wavelengths

Deltax = 1/N/Delta_phi; Deltay = 1/N/Delta_gamma;
horiz_x = [-N/2:N/2-1]*Deltax; horiz_y = [-N/2:N/2-1]*Deltay;
[x,y] = meshgrid(horiz_x,horiz_y);
r = sqrt(x.^2 + y.^2);

% create uniformly illuminated, circular aperture
f = zeros(size(x));
f(find(r<=D/2)) = 1;

% compute spatial frequencies
u = [-N/2:N/2-1]*(1/N)*(1/Delta_phi);
v = [-N/2:N/2-1]*(1/N)*(1/Delta_gamma);

% take absolute value squared of Fourier Transform to compute impulse
% response of circular aperture
F = fftshift( abs(fft2( fftshift(f) )).^2 );
F = F./prod(size(f));

% load in sky data
fid = fopen('hw8prob5data','rb');
data = fread(fid, inf, 'uint8');fclose(fid);
im = reshape(data, [N N]);

% part (a)

% convolve brightness image with impulse response

im2 = real(ifft2( fft2(im).*fft2( fftshift(F) ) ) );

% part (b)

% center locations of apertures
coords = [0 0; 0 0-150; 0 0+100;...
          0-100 0-100; 0+100 0-100];
coords = coords/lambda;

```

```

% create aperture array
map = zeros(size(x));
for k=1:size(coords,1)

    I = find( ( abs(x-coords(k,2))<=w/2) & ...
        ( abs(y-coords(k,1))<=w/2) );
    map(I) = 1;
end

% compute far-field power pattern of aperture array
H = fftshift( abs( fft2( fftshift(map) ) ).^2 );
H = H./prod(size(map));

% convolve brightness image with impulse response of aperture array
im3 = real(iff2( fft2(im).*fft2( fftshift(H) ) ));

% compute autocorrelation of aperture array
u = [-N/2:N/2-1]*(1/N)*(1/Delta_phi);
v = [-N/2:N/2-1]*(1/N)*(1/Delta_gamma);
autocorr_array = fftshift(real(iff2(fftshift(H))));
autocorr_circ = fftshift(real(iff2(fftshift(F))));

% plot out results
figure(1);
imagesc(Phi*180/pi,Gamma*180/pi,10*log10(im));
colormap bone; axis image;colorbar
h=gca;set(h,'FontSize',20);xlabel('degrees');
ylabel('degrees');

figure(2);
imagesc(Phi*180/pi,Gamma*180/pi,10*log10(im2));
colormap bone; axis image;colorbar
h=gca;set(h,'FontSize',20);xlabel('degrees');
ylabel('degrees');

```

```

figure(3);
imagesc(Phi*180/pi,Gamma*180/pi,10*log10(im3));
colormap bone; axis image;colorbar;
h=gca;set(h,'FontSize',20);xlabel('degrees');
ylabel('degrees');

% footprint of circular aperture autocorrelation
figure(4)
imagesc(u,v,autocorr_circ>1e-10);
colormap bone; axis image;caxis([0 1]);
h=gca;set(h,'FontSize',20);xlabel('cycles/rad');
ylabel('cycles/rad');

% footprint of antenna array autocorrelation
figure(5)
imagesc(u,v,autocorr_array>1e-10);
colormap bone; axis image;caxis([0 1]);
h=gca;set(h,'FontSize',20);xlabel('cycles/rad');
ylabel('cycles/rad');

```